Biosensors and Bioelectronics 142 (2019) 111489

Contents lists available at ScienceDirect

Biosensors and Bioelectronics

journal homepage: www.elsevier.com/locate/bios

# Futuristic medical implants using bioresorbable materials and devices

Suman Chatterjee[a], Mansi Saxena[a], Deepak Padmanabhan[b], Mahesh Jayachandra[c], Hardik J. Pandya[a,*]

[a] Biomedical and Electronic ($10^{-6}$-$10^{-9}$) Engineering Systems Laboratory, Department of Electronic Systems Engineering, Indian Institute of Science, Bangalore, 560012, India
[b] Sri Jayadeva Institute of Cardiovascular Sciences and Research, Bannerghatta Road, Bangalore, 560069, India
[c] Centre for BioSystems Science and Engineering, Indian Institute of Science, Bangalore, 560012, India

ARTICLE INFO

*Keywords:*
Bioresorbable materials
Sensor fabrication
Bioresorbable devices
Implantable devices
Clinical applications

ABSTRACT

Implantable medical devices have been used for real-time monitoring of physical parameters (temperature, pressure and biopotentials), sustained drug release, cardiovascular and pulmonary stents and other clinical applications. Several biocompatible materials (titanium and its alloys, aluminium, cobalt-alloys, stainless steel, poly-ethylene, polyurethanes, polyglycolide and polylactides) have been commercially used for fabricating implantable devices. However, these devices require retrieval operations after a certain period. Bioresorbable materials disintegrate gradually *in vivo* and their derivatives get absorbed completely in the body fluid with no residue and with minimal toxic effects, thus, eliminating the need for retrieval operations. In this article, state-of-the-art advances in materials, fabrication techniques and clinical applications of bioresorbable implantable devices are reviewed. We first discuss the bioresorbable materials (e.g., magnesium, molybdenum, tungsten, silicon, germanium, silicon dioxide, silicon nitride, silk and synthetic polymers) used in the fabrication of implantable devices. Later, an overview of processes to fabricate pressure, temperature, electrical and chemical sensors are discussed, followed by their applications as implantable devices in biomedical engineering.

## 1. Introduction

Implantable electronic devices for continuous monitoring of a subject without restricting movement are an integral part of modern healthcare systems. Such devices are used in various applications, from monitoring of post-operative status to daily vital parameters. As the implantable sensors are used for real-time measurement of parameters such as temperature, impedance, electrocardiogram, and respiratory rate (Kang et al., 2016), they have to be small, bio-compatible, reliable and sturdy enough to withstand the physical forces inside the body. Advances in microfabrication technology have facilitated wireless passive sensor systems, to offer real-time monitoring and treatment.

Microelectromechanical systems (MEMS) based technologies in implantable sensors have facilitated *in vivo* evaluations of various bodily parameters (Chen et al., 2010; Yu et al., 2016). Additionally, flexible implantable MEMS sensors have advantages in clinical practice because they allow continuous, real-time monitoring of patients and the ability to get help when a critical event occurs. The flexibility reduces local tissue damage and improves conformal contact with the physiological environment (Viventi et al., 2011). Sensing mechanisms in implantable MEMS-based sensors include electrochemical, mechanical or optical modalities. They can monitor pressure (Totsu et al., 2004; Troughton et al., 2011), temperature (Kang et al., 2016), pH (Cao et al., 2012), biopotentials (Griss et al., 2001), electrical impedance (Cao et al., 2012), flow (Chen and Lal, 2001; Hong et al., 1995) and concentration of oxygen (Mahutte, 1998) and glucose (Kim et al., 1999; Mastrototaro et al., 2006). Furthermore, implantable active sensors can transduce physiological input into electrical output.

Clinical applications of implantable sensors include diagnosis and monitoring of cardiovascular diseases (DiMarco, 2003; Hong et al., 1995; Langenfeld et al., 1998; Magalski et al., 2002), neuromotor diseases (Kipke et al., 2003; Schmidt et al., 1996; Zeng et al., 2008), brain signals (Yu et al., 2016), and muscle signals (Weir et al., 2009). Drug delivery is a novel application of implantable devices (Larrañeta et al., 2016; LaVan et al., 2003; Nguyen et al., 2013; Shawgo et al., 2002; Tesfamariam, 2018), where the dose of prescribed medicine is coupled to the recovery of the patient (Lee et al., 2015). Implanted electronic systems are used to stimulate nerves and to deliver drugs to the patient automatically at prescribed quantities and frequencies (Millard and Shepherd, 2007; Park et al., 2015). Pressure sensing has several significant clinical applications like arterial (DeHennis and Wise, 2006; Ritzema-Carter Jay L.T. et al., 2006; Schnakenberg et al., 2004),

* Corresponding author.
*E-mail address:* hjpandya@iisc.ac.in (H.J. Pandya).

https://doi.org/10.1016/j.bios.2019.111489
Received 13 April 2019; Received in revised form 19 June 2019; Accepted 29 June 2019
Available online 02 July 2019
0956-5663/ 

intracranial (Miyake et al., 1997; SIGNORINI et al., 1998) and intraocular (Chen et al., 2010; Twa et al., 2010) pressure monitoring. *Integrated Sensor Systems Inc. (ISSYS)* has developed a cylindrical monitoring device that can be inserted into the heart using a catheter to record real-time hemodynamic parameters (Bloss, 2016).

Permanent implanted electronic devices can lead to infection via percutaneous wires as well as biofilms formed on the device (Chamis et al., 2001; Hall-Stoodley et al., 2004). The surgical procedure to retrieve implanted devices can cause further complications due to re-operation (Hwang et al., 2012; Vajramani et al., 2005). Such processes are costly, need special tools and have increased morbidity and mortality. However, with advancement in materials, electronic circuit design technologies and state-of-the-art microfabrication procedures, a novel class of low-risk bioresorbable implantable devices and sensors have been fabricated and studied (Boutry et al., 2019; Kang et al., 2016; Kim et al., 2018; Shin et al., 2019; Yu et al., 2016). Research related to such devices involves hydrolysis of conductors, insulators, and semiconductors in body fluid (Hwang et al., 2013b; Jung et al., 2017; Kulkarni et al., 1966; Liu et al., 2015; Yin et al., 2014a). These implantable devices rely on complete dissolution of the device over a specific timeframe, eliminating complications of retrieval. The factors governing the dissolution of a fabricated device are the materials, its impurity concentration, device geometry, surface treatment and its site of implantation in the body (Anderson et al., 2003; Buchanan, 2008; Huang, 2018). Most of the reported bioresorbable MEMS-based devices are passive (Boutry et al., 2019; Kang et al., 2016; Yu et al., 2016), as incorporation of active elements requires an internal or external power source with bioresorbable circuitry.

Here, we review bioresorbable materials, fabrication techniques of minimally invasive bioresorbable implantable devices and their clinical applications. This article is divided into five sections. Section 1 (Introduction) describes the role of implantable sensors in clinical applications and advantages of using bioresorbable materials to fabricate the implantable sensors. Section 2 focuses on bioresorbable materials used to fabricate the sensors. Section 3 describes the process of fabricating pressure sensors, temperature sensors, electrical sensors and chemical sensors. Applications of fabricated bioresorbable sensors are in Section 4, followed by Section 5, where conclusion and future directions are discussed.

## 2. Bioresorbable materials

Hydrolysis and enzymatic degradation disintegrate the bioresorbable material in non-toxic products that eventually get dissolved without damaging surrounding tissues. The dissolved amount of material needs to be less than the body tolerance limit. The rate of dissolution depends on contact with body fluid, the flow of body fluid, temperature, crystal structure, crystal orientation and on the geometry of the material (Blasier et al., 1997; Yetkin et al., 1999). The dimensions of the fabricated device are designed based on the rate of dissolution of material in the body fluid.

Bioresorbable materials include metals, semiconductors, polymers, insulators, and nano-composites. Selection of materials for fabrication of implantable bioresorbable devices depends on their physical and chemical properties.

A typical sensor is fabricated on a substrate using sensing elements, metal interconnects and a protective encapsulation layer. Medical applications are challenging because the dissolution behaviour of the elements in the biological environment at a particular pH and temperature, governs the properties of the designed sensor.

### 2.1. Metals

Bioresorbable metals such as magnesium, zinc, tungsten, molybdenum, and iron (Liu et al., 2015; Yin et al., 2014a; Zhao et al., 2016) have been studied. A commonly used bioresorbable metal is magnesium (Mg), which is widely present in cells and participates in metabolic pathways. Unprotected Mg reacts with water to produce slowly dissolvable magnesium hydroxide ($Mg(OH)_2$), which further reacts with available $Cl^-$ ions to form highly soluble $MgCl_2$. The dissolution rate of Mg is determined as 4 μm/day and 1.7 μm/day in a solution of pH 12 and 7 (DI water) respectively at 37 °C (Kang et al., 2016). However, the higher dissolution rate of magnesium in biofluids limits its use to fabricate implantable devices. Hydrolysis mechanism of Mg in DI water or in biofluids is shown in equation (1) (Kang et al., 2016; Son et al., 2015).

$$Mg + H_2O\ (or\ aq.\ O_2) \rightarrow MgO + H_2O \rightarrow Mg(OH)_2 \quad (1)$$

Zinc shows uniform dissolution in biofluids at a lesser dissolution rate than magnesium. Thus, it can be used as a material for fabricating stents (SIGNORINI et al., 1998), scaffolds (Zhao et al., 2016) and electrodes for longer duration bioresorbable batteries (Yin et al., 2014a).

Molybdenum (Mo), a promising bioresorbable material, shows lower solubility in pure water than in an oxygen-rich environment. The dissolution rate of molybdenum is 20 nm/day and 7 nm/day in PBS (pH 7.4) and DI water (pH 7) respectively, ensuring longer function of an implanted device in aqueous medium (Kang et al., 2016). The dissolution chemistry of molybdenum is given in equation (2) (Kang et al., 2016). Molybdenum can be used as electrodes and interconnects to fabricate electronic devices.

$$2\,Mo + 3\,O_2 + 2\,H_2O \rightarrow 2\,H_2MoO_4 \quad (2)$$

Iron and tungsten are also commonly used bioresorbable metals. Studies show that thin film of iron and tungsten exhibit dissolution rates of 7 nm/day and 20 nm/day respectively in PBS (pH 7.4) (Lee et al., 2017, 2018; Orlowski and Rübben, 2011; Song et al., 2018; Yin et al., 2015). The dissolution chemistry of iron and tungsten in PBS is shown in equation (3) and equation (4) (Lee et al., 2017) respectively.

$$4\,Fe + 3\,O_2 + 10\,H_2O \rightarrow 4\,Fe(OH)_4^- + 4\,H^+ \quad (3)$$

$$W + 4\,H_2O \rightarrow WO_4^{2-} + 8\,H^+ + 6\,e^- \quad (4)$$

### 2.2. Semiconductors

In modern dissolvable electronics, semiconductors such as Si, Ge, and ZnO are commonly used owing to their compatibility with microengineering technologies as well as their tuneable electrical characteristics with different doping concentrations (Hwang et al., 2013c, 2012; Jung et al., 2017; Son et al., 2015). Due to the low dissolution rate in biofluids, Si and SiGe are used as nanomembranes and ZnO is used as nanowires. The dissolution chemistry of Si, Ge and ZnO are shown in equation (5), equation (6), and equation (7) (Jung et al., 2017) respectively.

$$Si + 4\,H_2O \rightarrow Si(OH)_4 + 2\,H_2 \quad (5)$$

$$Ge + H_2O + O_2\ (aq.\ ) \rightarrow H_2GeO_3(aq.\ ) \quad (6)$$

$$ZnO\ (s) + 2\,OH^- \rightarrow ZnO_2^{2-} + H_2O \quad (7)$$

Studies on complete hydrolysis of silicon show dependence on pH values, ionic concentrations and temperature. According to a study (Anderson et al., 2003) silicon dissolves faster in higher pH solution and rate of its dissolution increases with temperature. Experiments show varied dissolution rates for different crystalline structures. Amorphous Si (a-Si) dissolves faster than poly-crystalline Si because the reduced density of a-Si accelerates diffusion of the solution in the crystal. Similarly, a bulk of nano-porous Si (np-Si) exhibits much higher dissolution rate than Si nano-membrane (Si-NM) (Anderson et al., 2003). The dissolution rate of Si-NM and np-Si are reported as 23 nm/day and 9 μm/day in artificial cerebrospinal fluid (Kang et al., 2016).

### 2.3. Insulators

Insulators are used to insulate and encapsulate devices. Most of the bioresorbable insulators have low dissolution rates. Dissolution rate depends on porosity of the layer and density of materials. In silicon-based semiconductor industry, silicon dioxide and silicon nitride are the most widely used insulators and therefore, their hydrolysis is well studied (Hwang et al., 2012; Kang et al., 2014).

In bioresorbable electronics, the most common dielectric is $SiO_2$. It is used both for electrical insulation and device encapsulation. Hydrolysis of $SiO_2$ produces silicic acid or ortho-silicic acid ($Si(OH)_4$), which dissolves in biofluids. As the reaction of silicic acid production is catalysed by $OH^-$ ions, pH affects the dissolution rate (Finnie et al., 2009). The dissolution kinetics are also affected by concentration of ions (e.g., $K^+$, $Na^+$, $Ca^{+2}$ and $Mg^{+2}$) in biofluids (Kang et al., 2014). Moreover, $SiO_2$ obtained from different sources or processes exhibit different dissolution rates because of different densities. The dissolution rate of thermally grown oxide layer differs compared to deposited oxide layers. The dissolution rate for layers deposited by physical vapour deposition (PVD) and chemical vapour deposition (CVD) processes also different (Cheng, 2016; Kang et al., 2014). However, notwithstanding growth or deposition techniques, the hydrolysis of $SiO_2$ is the same and given in equation (8) (Kang et al., 2016).

$$SiO_2 + 2\,H_2O \rightarrow Si(OH)_4 \tag{8}$$

Another common inorganic insulating material used in bioresorbable electronics is silicon nitride. Dissolution of $Si_3N_4$ in biofluids happens in two steps. First, $SiO_2$ is generated from $Si_3N_4$ and next it is converted into silicic acid. The dissolution chemistry of $Si_3N_4$ is given by equation (9) (Huang, 2018).

$$Si_3N_4 + 12\,H_2O \rightarrow 3\,Si(OH)_4 + 4\,NH_3 \tag{9}$$

Due to generation of $SiO_2$ as an intermediate material in reaction, the dependence on temperature, pH and ion concentrations are similar to $SiO_2$ (Hwang et al., 2012).

Magnesium oxide (MgO) is also a potential candidate for an insulator in transient electronics. An intermediate compound $Mg(OH)_2$ is generated during dissolution of MgO in acidic or neutral solution (Mejias et al., 1999). The dissolution process of MgO depends on pH of the solution. Studies on these materials (Mg and MgO) suggest that they can dissolve in aqueous solution following a similar dissolution kinetics. Studies show that the dissolution rate for MgO is fastest among the materials discussed followed by $SiO_2$ and $Si_3N_4$. Additionally, the silicon dioxide grown using thermal evaporation showed a lower dissolution rate then grown using plasma enhanced chemical vapour deposition (PECVD) (Cheng, 2016; Huang, 2018).

### 2.4. Synthesized polymers

Biodegradable synthesized polymers such as, poly-lactic acid (PLA), poly-glycolic acid (PGA), poly-caprolactone (PCL), poly (1, 8 octanediol-*co*-citrate) (POC) and poly-lactic-*co*-glycolic acid (PLGA), a copolymer of PLA and PGA are widely used as substrates for transient electronics (Hwang et al., 2015, 2014). Interaction of these polymers with water decides the dissolution rate. The dissolution rate of hydrophilic polymers is higher than that of hydrophobic polymers. In 1966, Kulkarni et al. studied the biocompatibility of poly-L-lactic in animals (Kulkarni et al., 1966). The aliphatic polyesters as PLA(Cheng et al., 2009; Oksman et al., 2003; Rancan et al., 2009), PGA(Shawe et al., 2006), PLGA (Lü et al., 2009; Sarkar et al., 2006), and PCL(de Valence et al., 2012; Lee et al., 2003) are commonly used bioresorbable polymers. Among these polymers, PLA is one of the most widely used. Crystalline poly-l-lactic acid (PLLA) is mostly inert to hydrolysis, exhibiting low dissolution rate, whereas, hydrolysis-sensitive amorphous poly-dl-lactic acid (DL-PLA or PDLA) shows higher dissolution rate (Huang, 2018). Another commonly used polymer is PGA, which exhibits a higher rate of dissolution in biofluids than PLA. PLGA, a copolymer synthesized using PLA and PGA, is used widely in the fabrication of bioresorbable devices due to its tuneable properties, e.g., crystallinity, rate of dissolution, and hydrophobicity. By varying the ratio of PLA and PGA in PLGA, the rate of dissolution can be tuned to the desired value.

PCL, a bioresorbable aliphatic polyester exhibits much lower dissolution rate due to high crystallinity and hydrophobicity compared to PLA, PGA or PLGA (Hwang et al., 2013a). PCL is preferred as it is relatively easy to cast. Flexibility of PCL to be co-polymerized with other polymers like PLA or PLGA helps to achieve the desired properties. Unlike other polymers, POC is an elastomer and can be stretched up to 30% with linear mechanical response (Hwang et al., 2015). Thus, POC can be used to efficiently fabricate stretchable bioresorbable devices.

Unlike aliphatic polyesters, few polymers exhibit surface erosion, that means dissolution occurs layer by layer, resulting in better encapsulation performance. One of the most widely used such polymer is polyanhydride. Biocompatibility study shows that it is not cytotoxic. Moreover, the slow dissolution rate helps to protect the device by encapsulating from biofluids for a longer time (Kang et al., 2016).

### 2.5. Silk

Silk films can be used as substrates for bioresorbable devices. Silk is flexible, robust, and bioresorbable material (Anderson et al., 2003; Hwang et al., 2013a, 2013c; Kim et al., 2010, 2009) with a controllable period of dissolution and tuneable dissolution rate in an aqueous solution. Perry et al. developed a silk-fibroin based substrate fabrication technique by purification of *Bombyx mori* cocoons (Perry et al., 2008). The casting of silk-fibroin solution on a flat surface followed by drying, resulted in uniform silk films (Jung et al., 2017). Silk films are used as a substrate of electrophysiological recording electrodes and silicon-based transistor (Anderson et al., 2003; Kim et al., 2010, 2009). The bio-resorption process of silk film in water involves its proteolytic degradation, producing biocompatible materials (Horan et al., 2005). The dissolution rate can be varied by changing the rate of drying of silk solution (Lu et al., 2010), by reducing β content-sheet or by treatment of the film using ethanol (Kim et al., 2010) during film formation. Excellent bioresorbability and biocompatibility make silk a promising alternative for transient electronics.

Commonly used bioresorbable materials and processes used to fabricate a device using these materials are summarized in Table 1.

## 3. Fabrication of bioresorbable devices

Fabrication of bioresorbable implants has been made possible by advancements in material science and micro and nano fabrication technology. The implantable devices utilize conventional microfabrication compatible biosensors for sensing the change in physiological parameters (pressure, blood flow, pH, and biopotentials) of body and recording of biopotentials. Bioresorbable devices can be fabricated using conventional CMOS fabrication technology without significant retooling of systems and increase in cost.

### 3.1. Fabrication of pressure sensor

Silicon is the most commonly used substrate in pressure sensor fabrication. A fabricated deformable diaphragm structure of silicon nanomembrane can provide a highly sensitive pressure response. The most commonly used technology for sensing the force involves, measuring the deformations of the structure using piezoresistors. On applying a force to the piezoresistive sensor, the structure deforms and subjects to stress which results in a proportional change in the resistance of the sensor. A rapid, miniaturized, linear, and highly sensitive sensor with better resolution output can be fabricated using microengineering technologies. This change in resistance is then converted

**Table 1**
List of commonly used bioresorbable materials in transient electronics.

| Class | Materials | Fabrication processes used (growth or deposition) |
|---|---|---|
| Conductors | Mg, Zn, Mo, W (Yin et al., 2014a, 2014b) | E-beam evaporation |
| | Fe (Yin et al., 2014a) | Sputtering |
| | PGA, PLA, PLGA (Bettinger and Bao, 2010) | Melt and cast |
| | Silk (Anderson et al., 2003; Tao et al., 2014) | Cast |
| | Highly doped Si- nanomembrane (Yu et al., 2016) | Doping of Si wafer |
| Semiconductors | Si- nanomembrane (Anderson et al., 2003) | Si wafer, SOI wafer |
| | Poly-Si, amorphous Si(Yu et al., 2016) | LPCVD |
| | Ge (Jung et al., 2017) | Ge wafer |
| | ZnO(Dagdeviren et al., 2013) | Sputtering |
| Insulator | $SiO_2$(Hwang et al., 2015, 2012) | Thermal oxidation, PECVD, E-beam evaporation, ALD, Sputtering |
| | $Si_3N_4$(Hwang et al., 2012) | PECVD |
| | MgO(Anderson et al., 2003) | E-beam evaporation |
| | Polyanhydride (Kang et al., 2016) | Synthesis |
| Synthesized Polymers | PLA(Cheng et al., 2009; Oksman et al., 2003; Rancan et al., 2009) | Synthesis and Cast |
| | PGA(Shawe et al., 2006) | Synthesis and Cast |
| | PLGA (Lü et al., 2009; Sarkar et al., 2006) | Synthesis and Cast |

into electronic signals using signal conditioning circuits. The piezoresistive force sensors have higher sensitivity, noise immunity, with compact signal conditioning circuits compared to capacitive and piezoelectric type pressure sensors (Bakhoum and Cheng, 2010; Gerard Meijer et al., n.d.; Liu, 2012; Pandya et al., 2017; Yu and Huang, 2015).

The change in resistance of piezoresistive material is proportional to its gauge factor. Gauge factor of silicon, a function of doping and temperature, is high. Thus, as a piezoresistive material, it shows a significant change in resistance value. The piezoresistivity of silicon makes it potentially useful for fabricating pressure sensors. Schematics of piezoresistive pressure sensors and a temperature sensor are shown in Fig. 1.

In a piezoresistive pressure sensor, the piezoresistive material is placed on a deformable diaphragm structure so that it can experience a high average strain. The higher the value of the change in strain, the higher will be the sensitivity. The average strain in the silicon-nanomembrane structure on the deformable surface causes an electrical response. A PLGA diaphragm on np-Si structure can be used as a deformable structure (Fig. 1a). Finite element analysis shows that deformation of PLGA diaphragm is more (Kang et al., 2016), thus, validating its use as a pressure sensor. Here, piezoresistive material was placed at the centre of the edge of the diaphragm to maximize sensitivity.

In 2016, Kang et al. fabricated the device by integrating piezoresistive sensing element (highly doped Si-NM using solid-state diffusion of boron) onto PLGA and bonded it over a cavity etched into the np-Si substrate (Kang et al., 2016). First, a trench was created on the substrate to fabricate the cavity. $SiO_2$ layer was then deposited on the np-Si substrate followed by patterning and etching. Finally, np-Si substrate was etched to create the trench. The etch time controlled the depth of the trench according to the design. A parallel process flow was followed to get the sensing element. The top Si-NM layer was heavily

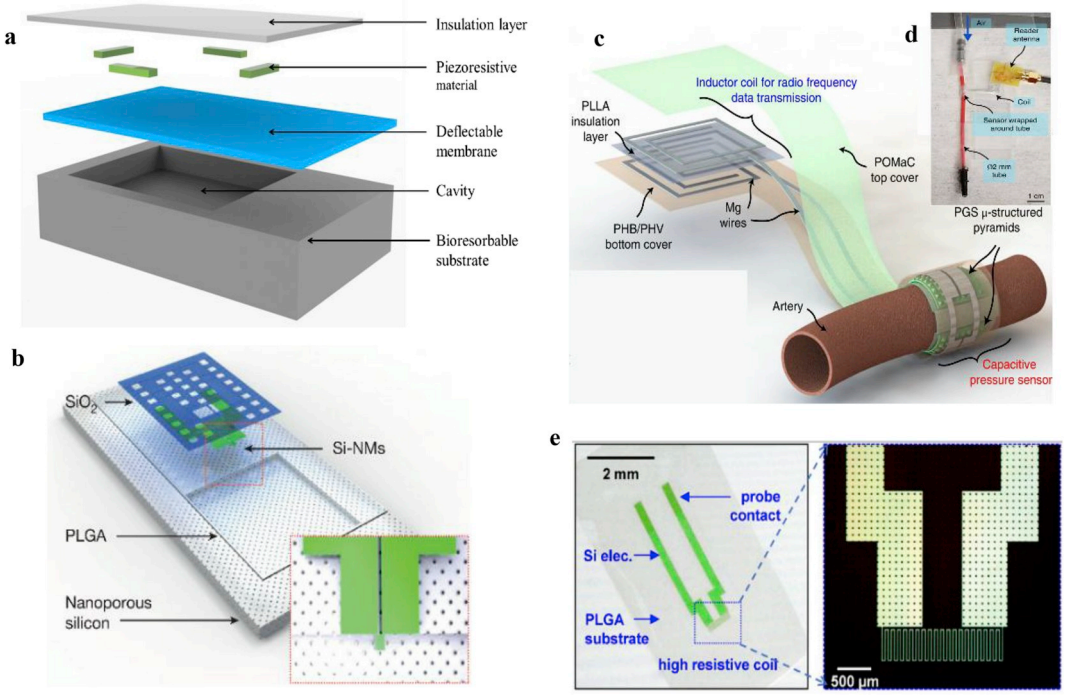


**Fig. 1. Bioresorbable pressure and temperature sensor**. **(a)** Schematic illustration of structure of a typical pressure sensor. **(b)** Schematic illustration of a bioresorbable pressure sensor on np-Si substrate with PLGA deflectable membrane and Si-NM sensing layer (Kang et al., 2016). **(c)** Illustration of the sensor with bilayer coil for wireless data transmission and capacitive pressor sensor wrapped around artery (Boutry et al., 2019). **(d)** Experimental setup to test fabricated sensor by mimicking pulsatile behaviour of an artery (Boutry et al., 2019). **(e)** Bioresorbable temperature sensor fabricated on PLGA film (Kang et al., 2016).

doped to achieve the expected sensitivity. Furthermore, it was dipped in hydrofluoric acid to release the top silicon layer by dissolving the buried oxide layer. The released layer was transferred on PLGA using a temporary carrier substrate. The PLGA structure was then bonded on the trench in the np-Si substrate and heated at a glass transition temperature, for 5 min on the hotplate, to form a cavity. Finally, the $SiO_2$ layer was deposited on Si-NM for insulation. Kang et al. reported pressure sensors with the np-Si and magnesium foil as substrates (Fig. 1b). Here, the sensing layer (highly boron-doped Si-NM) formed on a PLGA structure was bonded on a trench to form a cavity on the substrate (Kang et al., 2016).

A device for monitoring arterial-pulse was fabricated using biodegradable materials, e.g., magnesium, PLLA, POMaC and PHB/PHV (Boutry et al., 2019). The PGS was synthesized and poured into PDMS mould to fabricate square pyramidal micro-structures. Magnesium electrodes were fabricated using laser cut Mg foil. A PLLA insulator was used in between two magnesium layers. PHB/PHV was used to encapsulate the stack. The POMaC was synthesized and spin-coated to laminate the device (Fig. 1c). The device was fabricated on a wafer for easy-handling and could be peeled off easily after fabrication. The fabricated device could transmit the recorded signal by inductive coupling (Fig. 1d).

### 3.2. Fabrication of temperature sensor

For conductors, the change in resistance or conductance is linearly proportional to temperature. Temperature coefficient of resistance (TCR) of silicon can be tuned by varying dopant and doping concentration. This can be exploited to use doped Si for fabricating temperature sensors. Similarly, a thermal conductivity sensor can be fabricated using silicon nanomembrane structure. Increase in power to resistive elements increases temperature due to Joule heating. Analysis of temperature transients following the increase in power helps to determine thermal transport properties of surrounding fluid or tissue. A thin layer of silicon can be patterned as a temperature sensor, using the top silicon (highly doped) layer of an SOI wafer. The top layer can be spin-coated with a photoresist followed by patterning using lithography. Next, the top silicon layer can be etched using reactive ion etching (RIE) to pattern it as a temperature sensor. Similarly, a silicon nano-membrane layer on an insulated or non-conducting substrate can be patterned and etched to fabricate a silicon-based temperature sensor. Kang et al. reported fabrication of a temperature sensor (Fig. 1e) on a PLGA substrate using a heavily-doped Si-NM structure as electrode (Kang et al., 2016), whereas, Shin et al. reported fabrication of a temperature sensor by photolithography and RIE of the top silicon layer of an SOI wafer (Shin et al., 2019).

### 3.3. Fabrication of sensor for recording neural signals

The sensors for recording biopotentials transduce ionic concentration to electrical current. A passive electrode array can record biopotentials from a subject. In fabricating bioresorbable passive electrode array, bioresorbable metals are deposited and the device is fabricated on a bioresorbable substrate (np-Si, PLGA etc.). A thin layer of insulator is deposited to insulate the electrodes from substrate. The electrodes can be deposited by physical vapour deposition techniques, e.g., e-beam evaporation, sputtering or thermal evaporation. Insulation layer of silicon dioxide or silicon nitride can be deposited by chemical vapour deposition or physical deposition techniques. The deposited metal and insulator are patterned by photolithography. Schematics of chemical sensor and a device to record neural signals are shown in Fig. 2.

Kim et al. reported conformal dissolvable silk-based electrode array for recording brain signals. An array of thirty 500 μm square shaped gold electrodes was fabricated by transfer printing onto silk substrate. Yu et al. reported a bioresorbable device on PLGA substrate to record ECoG from brain (Yu et al., 2016). A metal-oxide-semiconductor structure was fabricated. The top layer of a SOI wafer was doped using phosphorus through patterned grown-oxide layer to define source and drain of NMOS structure that provides necessary buffer and switching actions. The releasing and transferring of the doped Si-NM was done using PI/PMMA bilayer on silicon wafer. Si-NM was patterned using photolithography and RIE. The $SiO_2$ layer deposited by PECVD, acted as gate dielectric. Sputtered molybdenum film was patterned using photolithography and lift-off process. This patterned film acts as gate electrodes and metal interconnects. An interlayer-dielectric was fabricated using tri-layer $SiO_2/Si_3N_4/SiO_2$ using PECVD. An additional layer of sensing electrodes and contact pads were fabricated by molybdenum deposition and patterning using lift-off and $SiO_2/Si_3N_4/SiO_2$ was deposited using PECVD as encapsulation layer with openings at electrode locations (Fig. 2a).

### 3.4. Chemical sensor

The chemical sensors have a wide range of applications in clinical monitoring. Amongst several applications of chemical sensors e.g., monitoring ionic compounds of blood or monitoring concentration of neurotransmitters, the pH monitoring and sensing biomolecules, e.g., blood glucose, protein have been widely used in biodegradable devices.

Schematic of a fabricated chemical sensor is shown in Fig. 2b. A silicon-based electrochemical sensor was designed and fabricated for detection of the concentration of dopamine (Kim et al., 2018). The device was fabricated on a biodegradable polycaprolactone (PCL) substrate, using iron decorated carboxylated polypyrrole nanoparticle ($Fe^{3+}$_CPPy NPs) coated silicon nanomembrane, as sensing layer (Fig. 2b). Magnesium was used for interconnects and electrodes, while silicon dioxide was used for electrical isolation. On a flexible substrate of PCL, a heavily doped Si-NM (~300 nm thick) was patterned as interdigitated electrodes and was coated with iron and carboxylated polypyrrole nanoparticles ($Fe^{3+}$_CPPy NPs) as a hybrid catalyst to fabricate an active sensing layer. Deposited magnesium (Mg~200 nm thick) layer acted as electrical contacts and interconnects and evaporated silicon dioxide ($SiO_2$~150 nm thick) served as interlayer dielectrics and protective layers. Polycaprolactone (100 μm thick) was used as substrate and encapsulant. The fabricated device can selectively sense dopamine to detect abnormalities in the nervous system.

The pH sensing is one of the most important applications of chemical sensors. Electrostatic gating of transport through Si-NM helps in pH sensor design. A functionalized surface of silicon-nanoribbon (Si-NR) can be used as a pH sensor. The change in surface charge density by depletion or accumulation of charge carriers changes the conductance (or resistance). This property can be used to monitor change in pH from changes in resistance. Kang et al. reported a silicon nanoribbon-based pH sensor (Kang et al., 2016). The silicon nanoribbons were exposed to UV induced ozone for 3 min followed by immersion in 1% ethanol solution of 3-aminopropyltriethoxysilane for 20 min. A thorough rinsing in ethanol followed by annealing of silicon nanoribbon at 60 °C for 10 min functionalized the surfaces. The functionalized surface with $–NH_2$ underwent protonation to $–NH_3^+$ at low pH and the -SiOH functionalized surface underwent deprotonation to $-SiO^-$ at high pH. The resulting change in conductance of phosphorus-doped Si-NR followed pH change of the solution. Increase in pH (pH 2 to pH 10) showed a step-wise decrease in conductance of phosphorus-doped Si-NR.

### 3.5. Energy storages

Implantable devices for clinical data recording require steady voltage for prolonged lifetimes. This can be accomplished by bioresorbable batteries. The bioresorbable energy storage devices are shown in Fig. 3. Lee et al. reported biodegradable micro-supercapacitor (Fig. 3a) which was fabricated using bioresorbable electrodes (tungsten, iron, and molybdenum) and hydrogel (agarose) electrolyte with NaCl salt. A

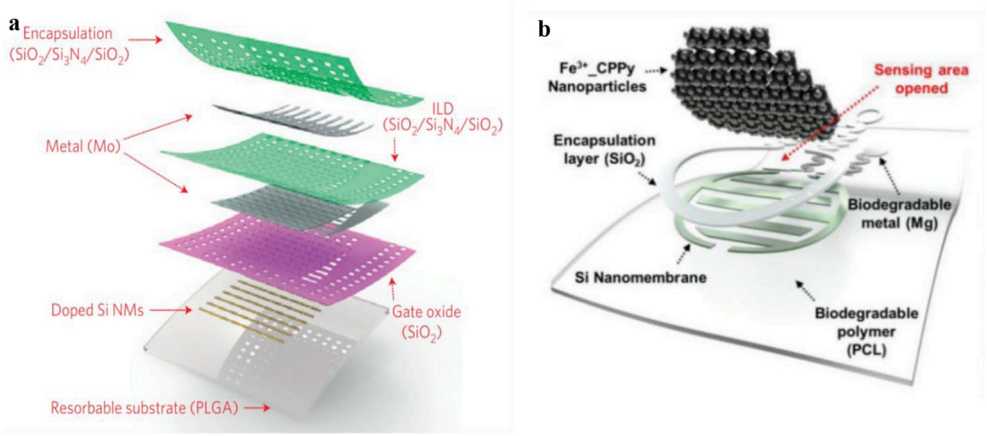


**Fig. 2. Bioresorbable electrical and chemical sensors**. **(a)** Exploded view of the schematic of fabricated bioresorbable sensor. The phosphorus doped Si-NM serves as neural interface electrodes (Yu et al., 2016). **(b)** Schematic of dopamine sensor on flexible polycaprolactone (PCL) substrate (thickness: 100 μm). The sensor consisted of ultrathin boron-doped Si-NM (~300 nm, released from SOI) with a coating of $Fe^{3+}$_CPPy NPs is the active sensing component and Mg (~200 nm) is used for electrical contacts and interconnects (Kim et al., 2018).

mixture of agarose powder and NaCl in DI water was heated, followed by cooling after pouring on a glass plate. This provided the electrolyte layer after detaching from the glass slide. Tungsten and molybdenum electrodes were deposited by magnetron sputtering and iron electrode was deposited by e-beam evaporation. The metal layers were patterned using lift-off process (Lee et al., 2017). Dissolution of the fabricated device was demonstrated in PBS (pH 7.4) at 37 °C after 9 days (Fig. 3b).

Huang et al. reported a Mg–$MoO_3$ battery (Fig. 3c). An active layer of $MoO_3$ powder mixed with PLGA resting on molybdenum foil acted as cathode, magnesium foil as anode and sodium alginate (ALG-Na) hydrogel with phosphate as electrolyte material. The electrolyte paste was cast on molybdenum film. The $MoO_3$ layer was deposited using magnetron sputtering. The battery was fabricated by stacking the electrodes and electrolytes and the structure was encapsulated using a polyanhydride layer (Huang et al., 2018). After implanting the device in rat, the complete dissolution was observed in a four weeks' time (Fig. 3d).

## 4. Applications of bioresorbable devices

In a preliminary study, Kim et al. (2009) showed that in animal models, silicon nanomembrane-based devices on a silk substrate could be dissolved in water and biofluids, without any toxicity. It was predicted that device fabrication using bioresorbable materials could be the future of biomedical devices (Kim et al., 2009). Hwang et al. reported the fabrication of bioresorbable transistors and simple circuits on silk substrate using magnesium as conductor and silicon dioxide and magnesium oxide as insulators in an encapsulating layer of silicon nitride (Hwang et al., 2013c). *In vivo* toxicity was determined with a subdermal implant in mouse and bioresorbability was tested in PBS solution.

Si-NM based pressure sensors are popular because of higher sensitivity due to their piezoresistivity. However, as piezoresistivity of a material is a function of temperature, to minimize sensitivity to change in temperature, a Wheatstone bridge configuration with four elements is used. The sensitivity of a piezoresistive sensor can be tuned by varying structure and dimension of silicon nanomembrane diaphragm. In 2016, Kang et al. reported an implantable, multifunctional device, fabricated using bioresorbable materials, making it resorbable in biofluid (ACSF). It could monitor intracranial pressure (Fig. 4a–d) and temperature during treatment of traumatic brain injury (Kang et al., 2016). The fabricated device was connected to a near-field communication (NFC) system using molybdenum wires. As, the exposed wire may act as source of infection, a device with on-chip transmission system could be a better option. Chen et al. studied a wireless, real-time pressure monitoring device and demonstrated recording of a human arterial pulse waveform from radial artery and *in vivo* monitoring of

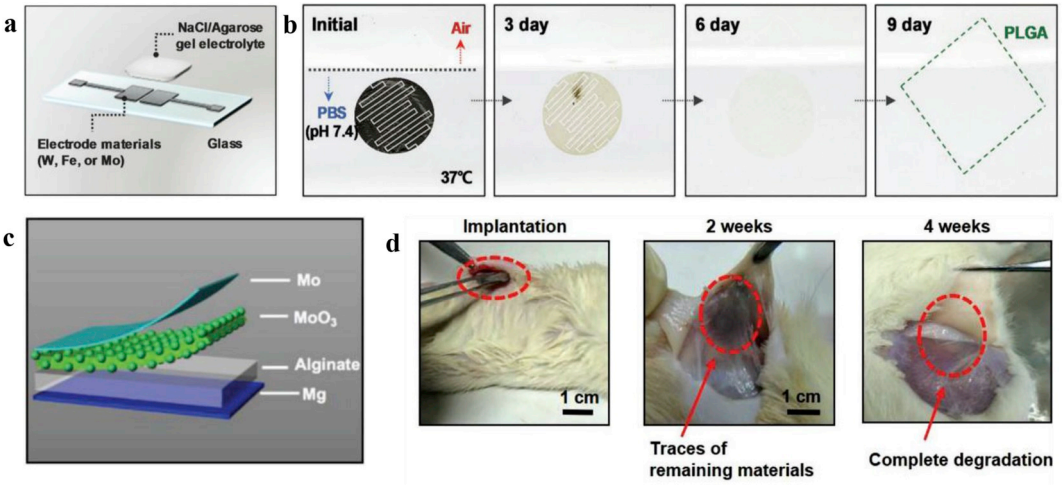


**Fig. 3. Bioresorbable power sources. (a)** Schematic illustration of a micro-supercapacitor consisting of bioresorbable metal (iron, tungsten or molybdenum) electrode using NaCl/Agarose gel as electrolyte on glass substrate. The electrodes are deposited on a film of 10 nm chromium for enhanced adhesion. The electrolyte is synthesized using NaCl and agarose powder in DI water (Lee et al., 2017). **(b)** Images of dissolution of electrodes in PBS solution (pH 7.4) at 37 °C at different times. **(c)** Schematic illustration of structure of the battery with materials. The paste cathode was made of $MoO_3$/Mo powder with PLGA (65:35) in acetone. Casting of this paste on Mo foil of 30 μm was followed by deposition of $MoO_3$ film of thickness ~1 μm. A film of UV-curable polyanhydride was used as encapsulation layer (Huang et al., 2018). **(d)** *in vivo* experiment of degradation of the battery by implanting in subcutaneous area (left) is shown with degradation after 2 weeks (center) and 4 weeks (right) of implantation.

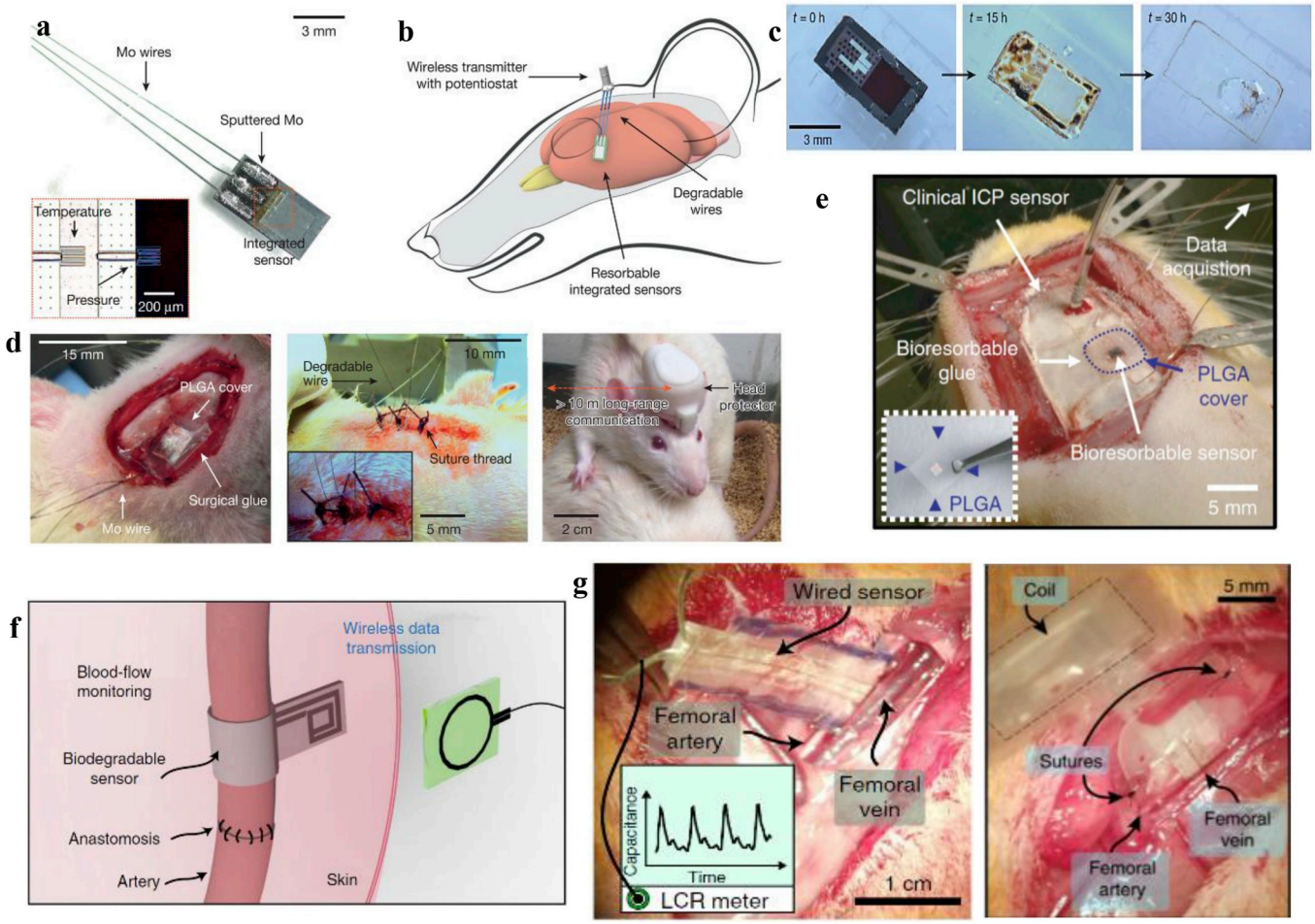


**Fig. 4. Bioresorbable pressor sensors**. **(a)** Image of intra-cranial pressure and temperature sensor with metal interconnects. The inset shows schematic of the sensor. **(b)** A diagram of reported sensor in intracranial space with external wireless data-transmission unit. **(c)** Validation of bioresorbability of the pressure sensor by accelerated dissolution into aqueous buffer solution of pH 12. **(d)** Implantation of bioresorbable sensor in rat, sealing the craniectomy defect by PLGA film and surgical glue and freely moving rat with wireless intracranial sensor (Kang et al., 2016). **(e)** Image of a bioresorbable sensor, implanted intra-cranially in rat. A strain gauge structure for the pressure sensing was fabricated using top silicon layer of SOI wafer. The device was fabricated by bonding it to another SOI wafer with trenches, using PDMS layer (Shin et al., 2019). **(f)** Illustration of post-operative monitoring of arterial pulsation. **(g)** Sites after implantation of pressure sensor with both wired and wireless mode of communication (Boutry et al., 2019). (For interpretation of the references to colour in this figure legend, the reader is referred to the Web version of this article.)

intracranial pressure in mice. Here, a fabricated pressure sensor was integrated with an inductive antenna to form a resonant circuit that could transmit a signal with shifted frequency, recorded by an external system (Chen et al., 2014).

A biodegradable PLLA-based pressure sensor was fabricated by Curry et al. to measure intra-organ pressures. The sensor was demonstrated by implanting into mouse abdomen to measure the diaphragmatic contraction pressure to detect the breathing pattern. The device used shear piezoelectricity of PLLA film to sense normal out-plane stress (Curry et al., 2018). Though the device could measure a wide range of pressure (0–18 KPa), it recorded reliable data only for four days. In 2018, Shin et al. reported bioresorbable pressure sensors to monitor chronic diseases and healing processes (Fig. 4e). This MRI-compatible monitoring device fabricated using bonded SOI wafers, was implanted in mice to measure intracranial pressure and dissolved in five weeks. The recorded signal for the first 25 days demonstrated high accuracy and was comparable to clinical-grade recordings (Shin et al., 2019). The encapsulation layer of silicon dioxide increased the lifetime of the fabricated device.

Boutry et al. demonstrated an implantable biodegradable sensor to measure strain and pressure with an *in vivo* experiment by implanting the sensor in rats. It used the capacitive effect to measure strain and pressure and a flexible capacitor to measure pressure. The change in capacitance between thin film comb electrodes was used to measure strain. The device was fabricated on PLLA substrate, with magnesium electrodes and poly (glycerol sebacate) or PGS dielectric layer using poly (octamethylene maleate (anhydride) citrate) or POMaC as packaging material. The device could measure pressure as well as the strain for 3.5 weeks after subcutaneous implantation (Boutry et al., 2018). The same group designed a sensor for wireless and battery-free monitoring of arterial pulse and blood flow through the artery as a part of real-time post-operative monitoring. The reported device was fabricated using bioresorbable materials like magnesium (as metal interconnect as well as inductor coil for radio frequency data transmission), PLLA (as insulation layer), POMaC (as top cover) and PHB/PHV (as bottom cover). The fabricated sensor was tested with a custom-made artificial artery model before *in vivo* testing in rats (Fig. 4f and g). The sensor showed partial degradation after 12 weeks, leaving behind PHB/PHV that had a slower degradation rate. Histological evaluations did not show severe inflammation around the site of implantation (Boutry et al., 2019).

As mentioned earlier, in 2016, Kang et al. reported an implantable, multifunctional device that could monitor intracranial pressure and temperature during traumatic brain injury (TBI) (Kang et al., 2016).

Shin et al. reported the use of temperature sensor in the monitoring of chronic diseases and healing (Shin et al., 2019).

Biopotentials, e.g., electrocardiogram, electromyogram, and electroencephalogram provide critical medical information for diagnosis and treatment. Biopotential electrodes, which can transduce bioelectric current derived from ionic transport in the body into electrical current, provide crucial metrics. The performance of non-invasive electrodes depends on electrode-skin impedance, i.e., to get a signal with high SNR, an implantable device is preferable.

Recording of biopotentials using the partially bioresorbable device for mapping feline brains was reported by Kim et al., in 2010. An array consisting of thirty 500 μm square shaped gold electrodes was fabricated by transfer printing onto a flexible and conformal silk substrate. The flexibility of silk facilitates conformal connection with the brain was efficiently demonstrated by *in vivo* neural monitoring. The response from visual cortex, with prominent visually evoked P100 responses and sleep spindles, was reported in this article (Kim et al., 2010). The fabricated device could only record signals from brain but any switching or multiplexing was not reported.

Similarly, Yu et al. reported recording of normal physiological and epileptiform activity from the brain (electrocorticography or ECoG) using implantable silicon-based devices for both acute and chronic rat models (Fig. 5). The implantable sensor was integrated with active multiplexing to capture data from a higher number of channels using switching and buffer transistors to minimize the number of transmission channels for recording high-resolution data. The acute experiments (~5–6 h) and chronic experiments (for 33 days) were performed on adult rats. Sleep spindle activity along with pre-ictal and inter-ictal signals were recorded from cortex in the left hemisphere and compared with the signals recorded by clinical grade electrodes. The fabricated bioresorbable device could record clinical grade significant data for a period of 33 days (depending on design) before getting dissolved in cerebrospinal fluid (Yu et al., 2016). Here, the recording electrodes were connected to outside NFC through a FET structure that allowed switching of recorded signal by control signals at gate terminal of FET.

The neural response from an animal model can be recorded using an electrode array placed on the brain surface, but microelectrodes (microneedles) can record data with high spatial resolution from specified depths of the brain. These probes are important in clinical applications owing to their stable and long-term functionality. Commercially available probes are much larger and stiffer than neurons. This limits their performance due to destruction of tissues in the brain during insertion of the device (Khilwani et al., 2016).

In 2014, Kozai et al. recorded chronic tissue responses in an *in vivo* study where microelectrodes, coated with bioresorbable carboxymethylcellulose were implanted in rats. The coating provided mechanical stiffness to the microneedle array (Kozai et al., 2014) and the needle was bioresorbable, but the probe was not. In 2016, Khilwani et al. reported a neural probe of a meander-shape platinum wire encapsulated with bioresorbable Parylene-C. A study in agarose gel after implantation of the probe showed complete dissolution of the Parylene-C layer of 1.1 μm thickness in 8 min leaving behind the electrodes with 0.5 μm thickness and 4 μm width (Fig. 6a–f). Also, dissolution of Parylene-C delivery needle was tested by implantation in bovine cadaver brain tissue (Khilwani et al., 2016). The delivery needle was completely bioresorbable while the recording electrode was not bioresorbable. The dissolution of microneedle (microelectrodes) minimizes scar tissue formation around the implant. A polyimide-based electrode array with a microneedle of acid-terminated PLGA as an insertion device for neural recording, was reported by Ceyssens et al., in 2019 (Fig. 6g and h). Here, an electrode array containing 16 electrodes with a diameter of 18 μm was arranged linearly with a 150 μm gap and inserted to a depth of 2.5 mm. A preliminary study of the mechanical properties was done in 0.6% agar gel that simulated a brain. Stable chronic neural recordings were demonstrated by implanting it in the sensorimotor cortex of rats to record evoked potentials and spontaneous action potentials for 4 months (Ceyssens et al., 2019).

Likewise, the recording of neural signals, the nervous system can be stimulated by electrical signals using bioresorbable devices. The first validation of a nonpharmacological neurogenerative study using bioresorbable devices was reported by J Koo et al. They reported an implantable, bioresorbable, wireless platform that can electrically

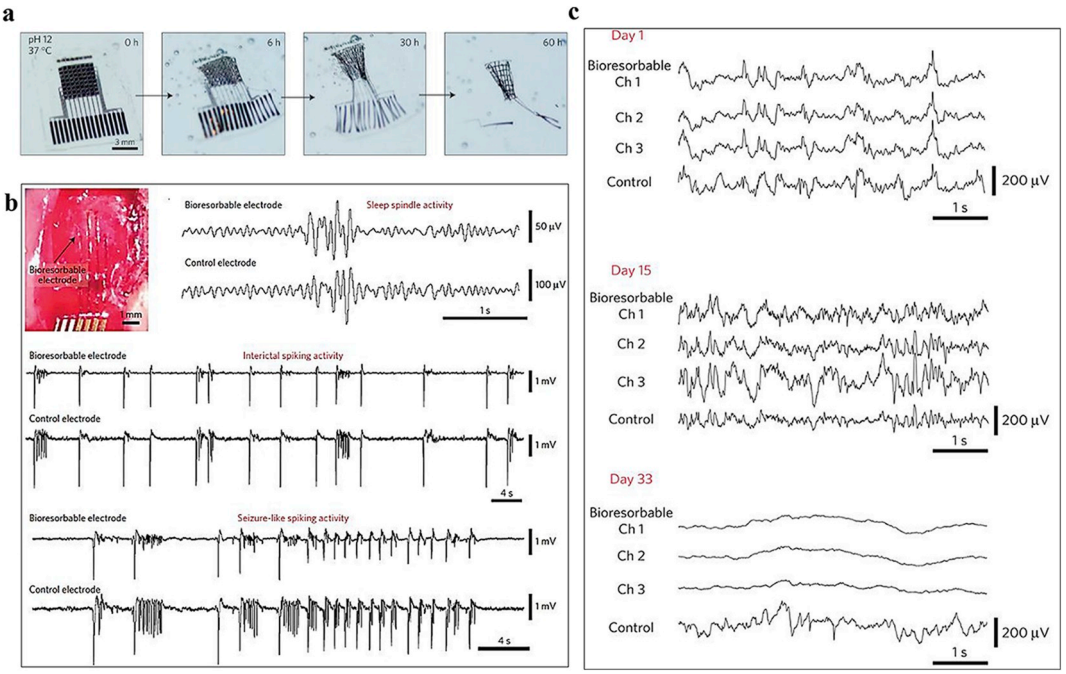


**Fig. 5. Bioresorbable sensor to record ECoG signal from rat brain. (a)** Images show the stages of accelerated dissolution of system immersed into aqueous buffer solution of pH 12 at 37 °C. **(b)** Image of a bioresorbable array of electrodes placed on the rat brain. Recorded signals from the left cortical surface, and sleep spindles from cortical surface. Interictal spiking activity was recorded 30 min after topical application of bicuculline methodide. A commercial stainless steel microwire electrode used as control. **(c)** Recorded ECoG signals by bioresorbable array and control electrode on day 1, day 15 and day 33 (Yu et al., 2016).

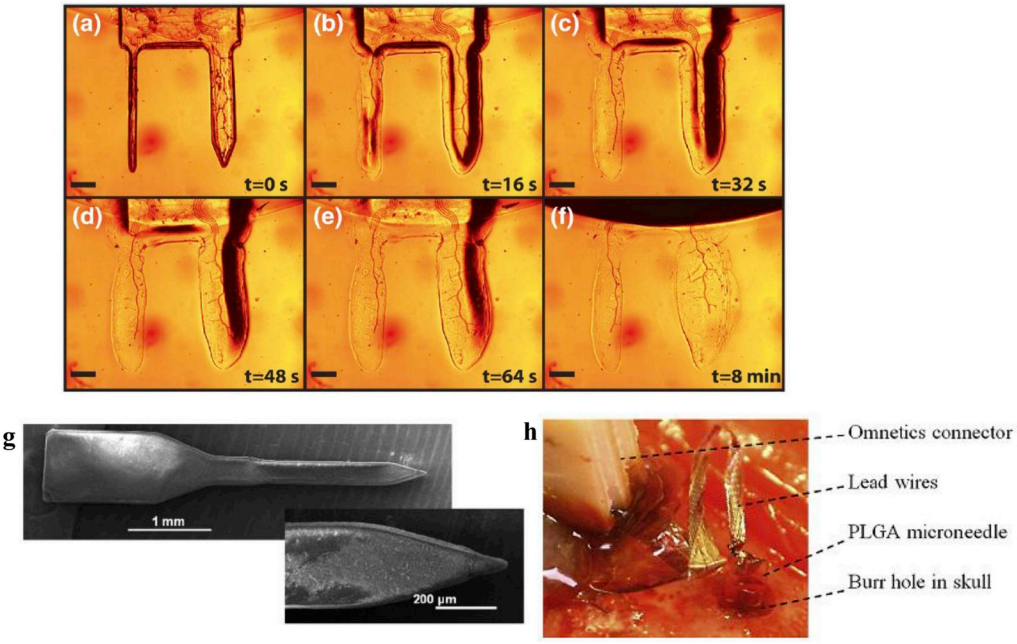


**Fig. 6. Bioresorbable materials in fabricating microneedle. (a)–(f)** Dissolution of fabricated microneedle in agarose gel at different times. The scale shown is 300 μm. The neural probe was fabricated by Parylene-C insulation on platinum wire. The insulation layer was shown to be dissolved in 8 min, leaving behind the platinum wire for electrical connectivity (Khilwani et al., 2016). **(g)** This image shows a PLGA microneedle fabricated by laser machining. **(h)** Photograph of implantation site of the PLGA microneedle (Ceyssens et al., 2019).

stimulate injured nerve tissues and results in improved nerve regeneration (Koo et al., 2018). The demonstrated device consists of an inductively coupled RF power harvester and electrical interface to nerve. The fabricated device was dissolved completely after 25 days in PBS at 37 °C. The experiment on dissolution of metal electrodes and wires in bovine serum at 37 °C showed an accelerated dissolution with the application of voltages. *In vivo* testing of the fabricated device in rodent model showed an enhanced axonal regeneration and recovery of the sciatic nerve. Moreover, terminal electromyography (EMG) signal showed an increase in muscle mass for tibialis anterior and exterior digitorum longus muscles by electrical stimulations.

Tao et al. demonstrated a subcutaneously implantable, silk-based bioresorbable therapeutic device that could be used to treat *in vivo Staphylococcus aureus* infection. The device was fabricated on a silk substrate using a resistor (for wireless heating) and a power receiving coil (for wireless inductive power transfer) of magnesium. The device was encapsulated in silk to increase its lifetime (Tao et al., 2014).

A multifunctional bioresorbable stent for treatment of cardiovascular diseases and a biomolecule sensor are shown in Fig. 7. Son et al. designed a multifunctional, implantable, bioresorbable endovascular electronic stent, integrated with therapeutic nanoparticles, which reduced inflammation (Fig. 7a). The flow sensor was designed to monitor blood flow with an integrated temperature sensor providing physiological signal sensing with controlled localized drug delivery. The integrated ceria nanoparticles and loaded drugs (e.g., rapamycin) helped catalytic reactive-oxygen-species scavenging and treatment of re-stenosis. The bioresorbable electronic stent was equipped with blood flow sensing (demonstrated by *ex vivo* experiment in the canine aorta) and data storage (in Mg/MgO/Mg structured memory cell) with transmitting antenna structure (Son et al., 2015). In 2018, Kim et al. fabricated a silicon-based flexible, bioresorbable, implantable electrochemical sensor for continuous, real-time monitoring of dopamine concentration to monitor nervous system disorders (Fig. 7b). An iron decorated carboxylated polypyrrole nanoparticle ($Fe^{3+}$_CPPy NPs) coated silicon nanomembrane based chemical sensor was used as a dopamine detector. Dopamine was converted to dopamine-o-quinone through catalytic oxidation by Fe-based nanoparticles. This reaction generated electrons that modulated electrical characteristics (Kim et al., 2018). However, it was reported that the device dissolved after 15 h, thereby, limiting its use for long term monitoring.

An on-board power source is critical to run these devices and transmit data for storage. In implantable devices, electrical stimulation and *in vivo* sensing applications are limited by a wired external power source or power transfer by near-field coupling. However,

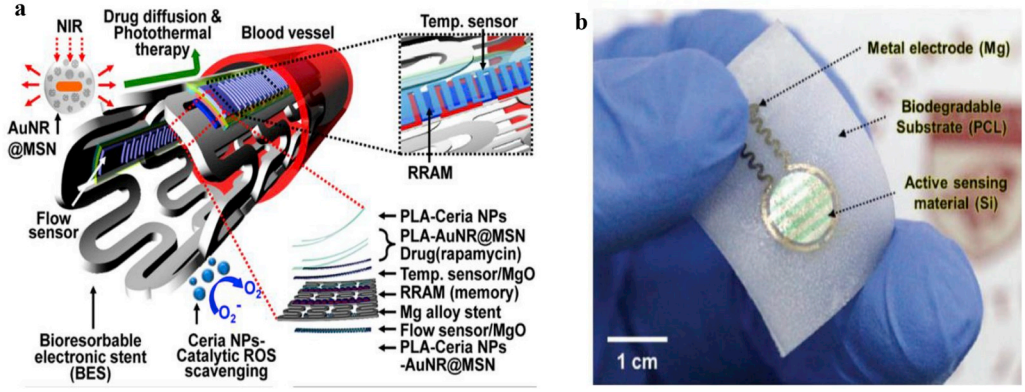


**Fig. 7. Bioresorbable sensors: a stent and a pH sensor. (a)** Design of bioresorbable multifunctional electronic stent integrated with nanoparticles for therapeutic applications. The stent includes temperature and flow sensor with memory modules and bioresorbable therapeutic nanoparticles. To fabricate this stent, an Mg-alloy ingot was laser cut followed by polishing. The stent was patterned using photolithography and an insulation layer of MgO was deposited. The memory unit was deposited by thermal evaporation (Mg) and sputtering (MgO). The temperature sensor was fabricated by deposition of Mg through shadow mask. The stent was laminated by PLA(Son et al., 2015). Reprinted (adapted) with permission. Copyright 2015 American Chemical Society. **(b)** Photograph of neurotransmitter (here dopamine) sensor on flexible polycaprolactone (PCL) substrate using $Fe^{3+}$_CPPy NPs sensing component (Kim et al., 2018).

commercially available batteries are not biodegradable and therefore, the biodegradable power supply remains as a challenge.

Douglas et al. developed a silicon-based, on-chip, triggered energy storage for transient electronics. The device was fabricated by deposition of vanadium oxide into porous silicon and PVA gel was used as an electrolyte. The charging/discharging cycles with cyclic voltammetry proved the efficiency of the device. With a trigger using NaOH solution (1 M), all active materials could be dissolved within 30 min (Douglas et al., 2016). In 2017, Lee et al. reported biodegradable micro-supercapacitors fabricated using transient materials with 500 charging/discharging cycles. The device was fabricated using bioresorbable electrodes (tungsten, iron, and molybdenum) and hydrogel (agarose) electrolyte with NaCl salt. A comparative study of electrochemical properties of proposed devices was reported (Lee et al., 2017). The fabricated device dissolved in nine days in PBS (at 37 °C) which implied this device could not be used for long durations. In 2018, a fully biodegradable magnesium and molybdenum-based battery was developed by Huang et al. to provide an on-board power source. The discharge behaviour of the fabricated Mg–$MoO_3$ battery could be tuned by the thickness of $MoO_3$ layer. The reported single cell Mg–$MoO_3$ battery provided a stable voltage output of 1.6 V. Along with degradation in PBS, an *in vivo* study in rats demonstrated complete degradation of the device in 4 weeks (Huang et al., 2018). The reported batteries were capable of powering ultra-low power devices for ECG signal detection, cardiac defibrillation, neural stimulation and recording, as well as pump small amounts of drugs (Amar et al., 2015; Demosthenous, 2014).

## 5. Conclusion

Conventional clinical procedures depend on implants for continuous long-term, real-time monitoring of physiological parameters and biopotentials. However, the implants cause irritation and leave scars after long-term use. Alternatively, transient devices can be used as implants to overcome these shortcomings.

In this article, bioresorbable materials, devices fabricated using the bioresorbable materials, and their applications are discussed.

Transient electronics technology or bioresorbable electronics devices offer innovative solutions that eliminate retrieval surgery for implants, thus, minimizing surgical-risks and generation of electronic waste. Although reported dissolvable devices show promising results, to commercialize these devices, relevant clinical studies are necessary to ensure biosafety and compliance.

The bioresorbable devices can be fabricated using conventional CMOS fabrication technology without significant changes in fabrication process. After implantation of a bioresorbable sensor in the subject, the dissolution mechanism starts as soon as sensor comes in contact with biofluids. Dimensions of the device are tuned based on the intended period of use, and the rate of dissolution. The advancement of research in material science will facilitate more controllable, triggered dissolution that deactivates the device or increases dissolution rate by stimulation using electrical signals, force or heat. The possibilities of improvement in mechanical and chemical properties of biomedical implants are mostly unexplored in bioresorbable electronics. Progressive development in implanted sensors to facilitate wireless connectivity, combined with IoT will help healthcare providers to monitor a patient remotely. A database consisting of signals recorded using bioresorbable sensors and standard clinical data can be referred to the healthcare provider in case of any emergency. Adding artificial intelligence will potentially improve the patient care by facilitating the development of self-supported bioresorbable clinical electronic systems for both diagnosis and monitoring.

## Conflict of interest

The authors declare no potential conflict of interest.

## Acknowledgement

Hardik J. Pandya acknowledges Indian Institute of Science, Bangalore for the start-up grant to establish the research and computational facilities at the Department of Electronic Systems Engineering.

## References

Amar, A.B., Kouki, A.B., Cao, H., 2015. Power approaches for implantable medical devices. Sensors 15, 28889–28914. https://doi.org/10.3390/s151128889.

Anderson, S.H.C., Elliott, H., Wallis, D.J., Canham, L.T., Powell, J.J., 2003. Dissolution of different forms of partially porous silicon wafers under simulated physiological conditions. Phys. Status Solidi 197, 331–335. https://doi.org/10.1002/pssa.200306519.

Bakhoum, E.G., Cheng, M.H.M., 2010. Novel capacitive pressure sensor. J. Microelectromech. Syst. 19, 443–450. https://doi.org/10.1109/JMEMS.2010.2047632.

Bettinger, C.J., Bao, Z., 2010. Organic thin-film transistors fabricated on resorbable biomaterial substrates. Adv. Mater. 22, 651–655. https://doi.org/10.1002/adma.200902322.

Blasier, R.D., Bucholz, R., Cole, W., Johnson, L.L., Mäkelä, E.A., 1997. Bioresorbable implants: applications in orthopaedic surgery. Instr. Course Lect. 46, 531–546.

Bloss, R., 2016. Embedded medical sensors, an emerging technology to monitor hearts, brains, nerves and addressing other medical applications for improved patient care. Sens. Rev. 36, 115–119. https://doi.org/10.1108/SR-11-2015-0184.

Boutry, C.M., Kaizawa, Y., Schroeder, B.C., Chortos, A., Legrand, A., Wang, Z., Chang, J., Fox, P., Bao, Z., 2018. A stretchable and biodegradable strain and pressure sensor for orthopaedic application. Nat. Electron. 1, 314. https://doi.org/10.1038/s41928-018-0071-7.

Boutry, C.M., Beker, L., Kaizawa, Y., Vassos, C., Tran, H., Hinckley, A.C., Pfattner, R., Niu, S., Li, J., Claverie, J., Wang, Z., Chang, J., Fox, P.M., Bao, Z., 2019. Biodegradable and flexible arterial-pulse sensor for the wireless monitoring of blood flow. Nat. Biomed. Eng. 3, 47. https://doi.org/10.1038/s41551-018-0336-5.

Buchanan, F.J., 2008. Degradation Rate of Bioresorbable Materials: Prediction and Evaluation. Elsevier.

Cao, H., Landge, V., Tata, U., Seo, Y., Rao, S., Tang, S., Tibbals, H.F., Spechler, S., Chiao, J., 2012. An implantable, batteryless, and wireless capsule with integrated impedance and pH sensors for gastroesophageal reflux monitoring. IEEE (Inst. Electr. Electron. Eng.) Trans. Biomed. Eng. 59, 3131–3139. https://doi.org/10.1109/TBME.2012.2214773.

Ceyssens, F., Bovet Carmona, M., Kil, D., Deprez, M., Tooten, E., Nuttin, B., Takeoka, A., Balschun, D., Kraft, M., Puers, R., 2019. Chronic neural recording with probes of subcellular cross-section using 0.06 $mm^2$ dissolving microneedles as insertion device. Sensor. Actuator. B Chem. 284, 369–376. https://doi.org/10.1016/j.snb.2018.12.030.

Chamis, A.L., Peterson, G.E., Cabell, C.H., Corey, G.R., Sorrentino, R.A., Greenfield, R.A., Ryan, T., Reller, L.B., Fowler, V.G., 2001. Staphylococcus aureus bacteremia in patients with permanent pacemakers or implantable cardioverter-defibrillators. Circulation 104, 1029–1033.

Chen, X., Lal, A., 2001. Integrated pressure and flow sensor in silicon-based ultrasonic surgical actuator. In: 2001 IEEE Ultrasonics Symposium. Proceedings. An International Symposium (Cat. No.01CH37263). Presented at the 2001 IEEE Ultrasonics Symposium. Proceedings. An International Symposium (Cat. No.01CH37263), vol. 2. pp. 1373–1376. https://doi.org/10.1109/ULTSYM.2001.991976.

Chen, P., Saati, S., Varma, R., Humayun, M.S., Tai, Y., 2010. Wireless intraocular pressure sensing using microfabricated minimally invasive flexible-coiled LC sensor implant. J. Microelectromech. Syst. 19, 721–734. https://doi.org/10.1109/JMEMS.2010.2049825.

Chen, L.Y., Tee, B.C.-K., Chortos, A.L., Schwartz, G., Tse, V.J., Lipomi, D., Wong, H.-S.P., McConnell, M.V., Bao, Z., 2014. Continuous wireless pressure monitoring and mapping with ultra-small passive sensors for health monitoring and critical care. Nat. Commun. 5, 5028. https://doi.org/10.1038/ncomms6028.

Cheng, H., 2016. Inorganic dissolvable electronics: materials and devices for biomedicine and environment. J. Mater. Res. 31, 2549–2570. https://doi.org/10.1557/jmr.2016.289.

Cheng, Y., Deng, S., Chen, P., Ruan, R., 2009. Polylactic acid (PLA) synthesis and modifications: a review. Front. Chem. China 4, 259–264. https://doi.org/10.1007/s11458-009-0092-x.

Curry, E.J., Ke, K., Chorsi, M.T., Wrobel, K.S., Miller, A.N., Patel, A., Kim, I., Feng, J., Yue, L., Wu, Q., Kuo, C.-L., Lo, K.W.-H., Laurencin, C.T., Ilies, H., Purohit, P.K., Nguyen, T.D., 2018. Biodegradable piezoelectric force sensor. Proc. Natl. Acad. Sci. Unit. States Am. 115, 909–914. https://doi.org/10.1073/pnas.1710874115.

Dagdeviren, C., Hwang, S.-W., Su, Y., Kim, S., Cheng, H., Gur, O., Haney, R., Omenetto, F.G., Huang, Y., Rogers, J.A., 2013. Transient, biocompatible electronics and energy harvesters based on ZnO. Small 9, 3398–3404. https://doi.org/10.1002/smll.201300146.

de Valence, S., Tille, J.-C., Mugnai, D., Mrowczynski, W., Gurny, R., Möller, M., Walpoth, B.H., 2012. Long term performance of polycaprolactone vascular grafts in a rat abdominal aorta replacement model. Biomaterials 33, 38–47. https://doi.org/10.1016/j.biomaterials.2011.09.024.

DeHennis, A.D., Wise, K.D., 2006. A fully integrated multisite pressure sensor for wireless arterial flow characterization. J. Microelectromech. Syst. 15, 678–685. https://doi.

org/10.1109/JMEMS.2006.876668.
Demosthenous, A., 2014. Advances in microelectronics for implantable medical devices. Adv. Electron. https://doi.org/10.1155/2014/981295.
DiMarco, J.P., 2003. Implantable cardioverter–defibrillators. N. Engl. J. Med. 349, 1836–1847. https://doi.org/10.1056/NEJMra035432.
Douglas, A., Muralidharan, N., Carter, R., Share, K.L., Pint, C., 2016. Ultrafast triggered transient energy storage by atomic layer deposition into porous silicon for integrated transient electronics. Nanoscale 8, 7384–7390. https://doi.org/10.1039/C5NR09095D.
Finnie, K.S., Waller, D.J., Perret, F.L., Krause-Heuer, A.M., Lin, H.Q., Hanna, J.V., Barbé, C.J., 2009. Biodegradability of sol–gel silica microparticles for drug delivery. J. Sol. Gel Sci. Technol. 49, 12–18. https://doi.org/10.1007/s10971-008-1847-4.
Griss, P., Enoksson, P., Tolvanen-Laakso, H.K., Merilainen, P., Ollmar, S., Stemme, G., 2001. Micromachined electrodes for biopotential measurements. J. Microelectromech. Syst. 10, 10–16. https://doi.org/10.1109/84.911086.
Hall-Stoodley, L., Costerton, J.W., Stoodley, P., 2004. Bacterial biofilms: from the Natural environment to infectious diseases. Nat. Rev. Microbiol. 2, 95–108. https://doi.org/10.1038/nrmicro821.
Hong, M.K., Wong, S.C., Mintz, G.S., Popma, J.J., Kent, K.M., Pichard, A.D., Satler, L.F., Leon, M.B., 1995. Can coronary flow parameters after stent placement predict restenosis. Cathet. Cardiovasc. Diagn. 36, 278–280. https://doi.org/10.1002/ccd.1810360321.
Horan, R.L., Antle, K., Collette, A.L., Wang, Y., Huang, J., Moreau, J.E., Volloch, V., Kaplan, D.L., Altman, G.H., 2005. In vitro degradation of silk fibroin. Biomaterials 26, 3385–3393. https://doi.org/10.1016/j.biomaterials.2004.09.020.
Huang, X., 2018. Materials and applications of bioresorbable electronics. J. Semicond. 39, 011003. https://doi.org/10.1088/1674-4926/39/1/011003.
Huang, X., Wang, D., Yuan, Z., Xie, W., Wu, Y., Li, R., Zhao, Y., Luo, D., Cen, L., Chen, B., Wu, H., Xu, H., Sheng, X., Zhang, M., Zhao, L., Yin, L., 2018. A fully biodegradable battery for self-powered transient implants. Small 14, 1800994. https://doi.org/10.1002/smll.201800994.
Hwang, S.-W., Tao, H., Kim, D.-H., Cheng, H., Song, J.-K., Rill, E., Brenckle, M.A., Panilaitis, B., Won, S.M., Kim, Y.-S., Song, Y.M., Yu, K.J., Ameen, A., Li, R., Su, Y., Yang, M., Kaplan, D.L., Zakin, M.R., Slepian, M.J., Huang, Y., Omenetto, F.G., Rogers, J.A., 2012. A physically transient form of silicon electronics. Science 337, 1640–1644. https://doi.org/10.1126/science.1226325.
Hwang, S.-W., Huang, X., Seo, J.-H., Song, J.-K., Kim, S., Hage-Ali, S., Chung, H.-J., Tao, H., Omenetto, F.G., Ma, Z., Rogers, J.A., 2013a. Materials for bioresorbable radio frequency electronics. Adv. Mater. 25, 3526–3531. https://doi.org/10.1002/adma.201300920.
Hwang, S.-W., Kim, D.-H., Tao, H., Kim, T., Kim, S., Yu, K.J., Panilaitis, B., Jeong, J.-W., Song, J.-K., Omenetto, F.G., Rogers, J.A., 2013b. Materials and fabrication processes for transient and bioresorbable high-performance electronics. Adv. Funct. Mater. 23, 4087–4093. https://doi.org/10.1002/adfm.201300127.
Hwang, S.-W., Kim, D.-H., Tao, H., Kim, T., Kim, S., Yu, K.J., Panilaitis, B., Jeong, J.-W., Song, J.-K., Omenetto, F.G., Rogers, J.A., 2013c. Materials and fabrication processes for transient and bioresorbable high-performance electronics. Adv. Funct. Mater. 23, 4087–4093. https://doi.org/10.1002/adfm.201300127.
Hwang, S.-W., Song, J.-K., Huang, X., Cheng, H., Kang, S.-K., Kim, B.H., Kim, J.-H., Yu, S., Huang, Y., Rogers, J.A., 2014. High-performance biodegradable/transient electronics on biodegradable polymers. Adv. Mater. 26, 3905–3911. https://doi.org/10.1002/adma.201306050.
Hwang, S.-W., Lee, C.H., Cheng, H., Jeong, J.-W., Kang, S.-K., Kim, J.-H., Shin, J., Yang, J., Liu, Z., Ameer, G.A., Huang, Y., Rogers, J.A., 2015. Biodegradable elastomers and silicon nanomembranes/nanoribbons for stretchable, transient electronics, and biosensors. Nano Lett. 15, 2801–2808. https://doi.org/10.1021/nl503997m.
Jung, Y.H., Zhang, H., Gong, S., Ma, Z., 2017. High-performance green semiconductor devices: materials, designs, and fabrication. Semicond. Sci. Technol. 32, 063002. https://doi.org/10.1088/1361-6641/aa6f88.
Kang, S.-K., Hwang, S.-W., Cheng, H., Yu, S., Kim, B.H., Kim, J.-H., Huang, Y., Rogers, J.A., 2014. Dissolution behaviors and applications of silicon oxides and nitrides in transient electronics. Adv. Funct. Mater. 24, 4427–4434. https://doi.org/10.1002/adfm.201304293.
Kang, S.-K., Murphy, R.K.J., Hwang, S.-W., Lee, S.M., Harburg, D.V., Krueger, N.A., Shin, J., Gamble, P., Cheng, H., Yu, S., Liu, Z., McCall, J.G., Stephen, M., Ying, H., Kim, J., Park, G., Webb, R.C., Lee, C.H., Chung, S., Wie, D.S., Gujar, A.D., Vemulapalli, B., Kim, A.H., Lee, K.-M., Cheng, J., Huang, Y., Lee, S.H., Braun, P.V., Ray, W.Z., Rogers, J.A., 2016. Bioresorbable silicon electronic sensors for the brain. Nature 530, 71–76. https://doi.org/10.1038/nature16492.
Khilwani, R., Gilgunn, P.J., Kozai, T.D.Y., Ong, X.C., Korkmaz, E., Gunalan, P.K., Cui, X.T., Fedder, G.K., Ozdoganlar, O.B., 2016. Ultra-miniature ultra-compliant neural probes with dissolvable delivery needles: design, fabrication and characterization. Biomed. Microdevices 18, 97. https://doi.org/10.1007/s10544-016-0125-4.
Kim, Y.T., Kim, Y.-Y., Jun, C.-H., 1999. Needle-shaped glucose sensor with multicell electrode fabricated by surface micromachining. In: Design, Test, and Microfabrication of MEMS and MOEMS. Presented at the Design, Test, and Microfabrication of MEMS and MOEMS. International Society for Optics and Photonics, pp. 924–931. https://doi.org/10.1117/12.341159.
Kim, D.-H., Kim, Y.-S., Amsden, J., Panilaitis, B., Kaplan, D.L., Omenetto, F.G., Zakin, M.R., Rogers, J.A., 2009. Silicon electronics on silk as a path to bioresorbable, implantable devices. Appl. Phys. Lett. 95, 133701. https://doi.org/10.1063/1.3238552.
Kim, D.-H., Viventi, J., Amsden, J.J., Xiao, J., Vigeland, L., Kim, Y.-S., Blanco, J.A., Panilaitis, B., Frechette, E.S., Contreras, D., Kaplan, D.L., Omenetto, F.G., Huang, Y., Hwang, K.-C., Zakin, M.R., Litt, B., Rogers, J.A., 2010. Dissolvable films of silk fibroin for ultrathin conformal bio-integrated electronics. Nat. Mater. 9, 511–517. https://doi.org/10.1038/nmat2745.
Kim, Hyun-Seung, Yang, S.M., Jang, T.-M., Oh, N., Kim, Hee-Soo, Hwang, S.-W., 2018. Bioresorbable silicon nanomembranes and iron catalyst nanoparticles for flexible, transient electrochemical dopamine monitors. Adv. Healthc. Mater. 7, 1801071. https://doi.org/10.1002/adhm.201801071.
Kipke, D.R., Vetter, R.J., Williams, J.C., Hetke, J.F., 2003. Silicon-substrate intracortical microelectrode arrays for long-term recording of neuronal spike activity in cerebral cortex. IEEE Trans. Neural Syst. Rehabil. Eng. 11, 151–155. https://doi.org/10.1109/TNSRE.2003.814443.
Koo, J., MacEwan, M.R., Kang, S.-K., Won, S.M., Stephen, M., Gamble, P., Xie, Z., Yan, Y., Chen, Y.-Y., Shin, J., Birenbaum, N., Chung, S., Kim, S.B., Khalifeh, J., Harburg, D.V., Bean, K., Paskett, M., Kim, J., Zohny, Z.S., Lee, S.M., Zhang, R., Luo, K., Ji, B., Banks, A., Lee, H.M., Huang, Y., Ray, W.Z., Rogers, J.A., 2018. Wireless bioresorbable electronic system enables sustained nonpharmacological neuroregenerative therapy. Nat. Med. 24, 1830–1836. https://doi.org/10.1038/s41591-018-0196-2.
Kozai, T.D.Y., Gugel, Z., Li, X., Gilgunn, P.J., Khilwani, R., Ozdoganlar, O.B., Fedder, G.K., Weber, D.J., Cui, X.T., 2014. Chronic tissue response to carboxymethyl cellulose based dissolvable insertion needle for ultra-small neural probes. Biomaterials 35, 9255–9268. https://doi.org/10.1016/j.biomaterials.2014.07.039.
Kulkarni, R.K., Pani, K.C., Neuman, C., Leonard, F., 1966. Polylactic acid for surgical implants. Arch. Surg. 93, 839–843. https://doi.org/10.1001/archsurg.1966.01330050143023.
Langenfeld, H., Krein, A., Kirstein, M., Binner, L., 1998. Peak endocardial acceleration-based clinical testing of the “BEST” DDDR pacemaker. Pacing Clin. Electrophysiol. 21, 2187–2191. https://doi.org/10.1111/j.1540-8159.1998.tb01150.x.
Larrañeta, E., Lutton, R.E.M., Woolfson, A.D., Donnelly, R.F., 2016. Microneedle arrays as transdermal and intradermal drug delivery systems: materials science, manufacture and commercial development. Mater. Sci. Eng. R Rep. 104, 1–32. https://doi.org/10.1016/j.mser.2016.03.001.
LaVan, D.A., McGuire, T., Langer, R., 2003. Small-scale systems for *in vivo* drug delivery. Nat. Biotechnol. 21, 1184–1191. https://doi.org/10.1038/nbt876.
Lee, K.H., Kim, H.Y., Khil, M.S., Ra, Y.M., Lee, D.R., 2003. Characterization of nano-structured poly(ε-caprolactone) nonwoven mats via electrospinning. Polymer 44, 1287–1294. https://doi.org/10.1016/S0032-3861(02)00820-0.
Lee, C.H., Kim, H., Harburg, D.V., Park, G., Ma, Y., Pan, T., Kim, J.S., Lee, N.Y., Kim, B.H., Jang, K.-I., Kang, S.-K., Huang, Y., Kim, J., Lee, K.-M., Leal, C., Rogers, J.A., 2015. Biological lipid membranes for on-demand, wireless drug delivery from thin, bioresorbable electronic implants. NPG Asia Mater. 7 e227–e227. https://doi.org/10.1038/am.2015.114.
Lee, G., Kang, S.-K., Won, S.M., Gutruf, P., Jeong, Y.R., Koo, J., Lee, S.-S., Rogers, J.A., Ha, J.S., 2017. Fully biodegradable microsupercapacitor for power storage in transient electronics. Adv. Energy Mater. 7, 1700157. https://doi.org/10.1002/aenm.201700157.
Lee, S., Koo, J., Kang, S.-K., Park, G., Lee, Y.J., Chen, Y.-Y., Lim, S.A., Lee, K.-M., Rogers, J.A., 2018. Metal microparticle – polymer composites as printable, bio/ecoresorbable conductive inks. Mater. Today 21, 207–215. https://doi.org/10.1016/j.mattod.2017.12.005.
Liu, C., 2012. Foundations of MEMS, second ed. Prentice Hall, Upper Saddle River, N.J.
Liu, X., Sun, J., Yang, Y., Pu, Z., Zheng, Y., 2015. In vitro investigation of ultra-pure Zn and its mini-tube as potential bioabsorbable stent material. Mater. Lett. 161, 53–56. https://doi.org/10.1016/j.matlet.2015.06.107.
Lü, J.-M., Wang, X., Marin-Muller, C., Wang, H., Lin, P.H., Yao, Q., Chen, C., 2009. Current advances in research and clinical applications of PLGA-based nanotechnology. Expert Rev. Mol. Diagn. 9, 325–341. https://doi.org/10.1586/erm.09.15.
Lu, Q., Hu, X., Wang, X., Kluge, J.A., Lu, S., Cebe, P., Kaplan, D.L., 2010. Water-insoluble silk films with silk I structure. Acta Biomater. 6, 1380–1387. https://doi.org/10.1016/j.actbio.2009.10.041.
Magalski, A., Adamson, P., Gadler, F., Böehm, M., Steinhaus, D., Reynolds, D., Vlach, K., Linde, C., Cremers, B., Sparks, B., Bennett, T., 2002. Continuous ambulatory right heart pressure measurements with an implantable hemodynamic monitor: a multicenter, 12-month follow-up study of patients with chronic heart failure. J. Card. Fail. 8, 63–70. https://doi.org/10.1054/jcaf.2002.32373.
Mahutte, C.K., 1998. On-line arterial blood gas analysis with optodes: current status. Clin. Biochem. 31, 119–130. https://doi.org/10.1016/S0009-9120(98)00009-5.
Mastrototaro, J.J., Cooper, K.W., Soundararajan, G., Sanders, J.B., Shah, R.V., 2006. Clinical experience with an integrated continuous glucose sensor/insulin pump platform: a feasibility study. Adv. Ther. 23, 725–732. https://doi.org/10.1007/BF02850312.
Gerard Meijer, Michiel Pertijs, Kofi Makinwa, n.d. Smart Sensor Systems. Wiley. https://doi.org/10.1002/9780470866931.
Mejias, J.A., Berry, A.J., Refson, K., Fraser, D.G., 1999. The kinetics and mechanism of MgO dissolution. Chem. Phys. Lett. 314, 558–563. https://doi.org/10.1016/S0009-2614(99)00909-4.
Millard, R.E., Shepherd, R.K., 2007. A fully implantable stimulator for use in small laboratory animals. J. Neurosci. Methods 166, 168–177. https://doi.org/10.1016/j.jneumeth.2007.07.009.
Miyake, H., Ohta, T., Kajimoto, Y., Matsukawa, M., Miyake, H., 1997. A new ventriculoperitoneal shunt with a telemetric intracranial pressure sensor: clinical experience in 94 patients with hydrocephalus. Neurosurgery 40, 931–935. https://doi.org/10.1097/0006123-199705000-00009.
Nguyen, N.-T., Shaegh, S.A.M., Kashaninejad, N., Phan, D.-T., 2013. Design, fabrication and characterization of drug delivery systems based on lab-on-a-chip technology. Adv. Drug Deliv. Rev. 65, 1403–1419. https://doi.org/10.1016/j.addr.2013.05.008.
Oksman, K., Skrifvars, M., Selin, J.-F., 2003. Natural fibres as reinforcement in polylactic acid (PLA) composites. Compos. Sci. Technol. Eco-Compos. 63, 1317–1324. https://

doi.org/10.1016/S0266-3538(03)00103-9.
Orlowski, M., Rübben, A., 2011. Bioresorbable Metal Stent with Controlled Resorption. US20110076319A1.
Pandya, H.J., Sheng, J., Desai, J.P., 2017. MEMS-based flexible force sensor for tri-axial catheter contact force measurement. J. Microelectromech. Syst. 26, 264–272. https://doi.org/10.1109/JMEMS.2016.2636018.
Park, S.I., Brenner, D.S., Shin, G., Morgan, C.D., Copits, B.A., Chung, H.U., Pullen, M.Y., Noh, K.N., Davidson, S., Oh, S.J., Yoon, J., Jang, K.-I., Samineni, V.K., Norman, M., Grajales-Reyes, J.G., Vogt, S.K., Sundaram, S.S., Wilson, K.M., Ha, J.S., Xu, R., Pan, T., Kim, T., Huang, Y., Montana, M.C., Golden, J.P., Bruchas, M.R., Gereau, R.W., Rogers, J.A., 2015. Soft, stretchable, fully implantable miniaturized optoelectronic systems for wireless optogenetics. Nat. Biotechnol. 33, 1280–1286. https://doi.org/10.1038/nbt.3415.
Perry, H., Gopinath, A., Kaplan, D.L., Negro, L.D., Omenetto, F.G., 2008. Nano- and micropatterning of optically transparent, mechanically robust, biocompatible silk fibroin films. Adv. Mater. 20, 3070–3072. https://doi.org/10.1002/adma.200800011.
Rancan, F., Papakostas, D., Hadam, S., Hackbarth, S., Delair, T., Primard, C., Verrier, B., Sterry, W., Blume-Peytavi, U., Vogt, A., 2009. Investigation of polylactic acid (PLA) nanoparticles as drug delivery systems for local dermatotherapy. Pharm. Res. (N. Y.) 26, 2027–2036. https://doi.org/10.1007/s11095-009-9919-x.
Ritzema-Carter Jay, L.T., Smyth, David, Troughton Richard, W., Crozier Ian, G., Melton Iain, C., Richards A, Mark, Neal, Eigler, James, Whiting, Kar, Saibal, Henry, Krum, Abraham William, T., 2006. Dynamic myocardial ischemia caused by circumflex artery stenosis detected by a new implantable left atrial pressure monitoring device. Circulation 113, e705–e706. https://doi.org/10.1161/CIRCULATIONAHA.105.572040.
Sarkar, S., Lee, G.Y., Wong, J.Y., Desai, T.A., 2006. Development and characterization of a porous micro-patterned scaffold for vascular tissue engineering applications. Biomaterials 27, 4775–4782. https://doi.org/10.1016/j.biomaterials.2006.04.038.
Schmidt, E.M., Bak, M.J., Hambrecht, F.T., Kufta, C.V., O'Rourke, D.K., Vallabhanath, P., 1996. Feasibility of a visual prosthesis for the blind based on intracortical micro stimulation of the visual cortex. Brain 119, 507–522. https://doi.org/10.1093/brain/119.2.507.
Schnakenberg, U., Krüger, C., Pfeffer, J.-G., Mokwa, W., vom Bögel, G., Günther, R., Schmitz-Rode, T., 2004. Intravascular Pressure Monitoring System. Sensors and Actuators A: Physical, Selected Papers from Eurosensors XVI Prague, Czech Republic, vol. 110. pp. 61–67. https://doi.org/10.1016/j.sna.2003.04.001.
Shawe, S., Buchanan, F., Harkin-Jones, E., Farrar, D., 2006. A study on the rate of degradation of the bioabsorbable polymer polyglycolic acid (PGA). J. Mater. Sci. 41, 4832–4838. https://doi.org/10.1007/s10853-006-0064-1.
Shawgo, R.S., Richards Grayson, A.C., Li, Y., Cima, M.J., 2002. BioMEMS for drug delivery. Curr. Opin. Solid State Mater. Sci. 6, 329–334. https://doi.org/10.1016/S1359-0286(02)00032-3.
Shin, J., Yan, Y., Bai, W., Xue, Y., Gamble, P., Tian, L., Kandela, I., Haney, C.R., Spees, W., Lee, Y., Choi, M., Ko, J., Ryu, H., Chang, J.-K., Pezhouh, M., Kang, S.-K., Won, S.M., Yu, K.J., Zhao, J., Lee, Y.K., MacEwan, M.R., Song, S.-K., Huang, Y., Ray, W.Z., Rogers, J.A., 2019. Bioresorbable pressure sensors protected with thermally grown silicon dioxide for the monitoring of chronic diseases and healing processes. Nat. Biomed. Eng. 3, 37. https://doi.org/10.1038/s41551-018-0300-4.
SIGNORINI, D.F., SHAD, A., PIPER, I.R., STATHAM, P.F.X., 1998. A clinical evaluation of the Codman MicroSensor for intracranial pressure monitoring. Br. J. Neurosurg. 12, 223–227. https://doi.org/10.1080/02688699845032.
Son, D., Lee, J., Lee, D.J., Ghaffari, R., Yun, S., Kim, S.J., Lee, J.E., Cho, H.R., Yoon, S., Yang, S., Lee, S., Qiao, S., Ling, D., Shin, S., Song, J.-K., Kim, Jaemin, Kim, T., Lee, H., Kim, Jonghoon, Soh, M., Lee, N., Hwang, C.S., Nam, S., Lu, N., Hyeon, T., Choi, S.H., Kim, D.-H., 2015. Bioresorbable electronic stent integrated with therapeutic nanoparticles for endovascular diseases. ACS Nano 9, 5937–5946. https://doi.org/10.1021/acsnano.5b00651.
Song, F., Wang, H., Sun, J., Gao, H., Wu, S., Yang, M., Ma, X., Hao, Y., 2018. ZnO-based physically transient and bioresorbable memory on silk protein. IEEE Electron. Device Lett. 39, 31–34. https://doi.org/10.1109/LED.2017.2774842.
Tao, H., Hwang, S.-W., Marelli, B., An, B., Moreau, J.E., Yang, M., Brenckle, M.A., Kim, S., Kaplan, D.L., Rogers, J.A., Omenetto, F.G., 2014. Silk-based resorbable electronic devices for remotely controlled therapy and in vivo infection abatement. Proc. Natl. Acad. Sci. Unit. States Am. 111, 17385–17389. https://doi.org/10.1073/pnas.1407743111.
Tesfamariam, B., 2018. Bioresorbable scaffold-based controlled drug delivery for restenosis. J. Cardiovasc. Transl. Res. https://doi.org/10.1007/s12265-018-9841-x.
Totsu, K., Haga, Y., Esashi, M., 2004. Ultra-miniature fiber-optic pressure sensor using white light interferometry. J. Micromech. Microeng. 15, 71–75. https://doi.org/10.1088/0960-1317/15/1/011.
Troughton, R.W., Ritzema, J., Eigler, N.L., Melton, I.C., Krum, H., Adamson, P.B., Kar, S., Shah, P.K., Whiting, J.S., Heywood, J.T., Rosero, S., Singh, J.P., Saxon, L., Matthews, R., Crozier, I.G., Abraham, W.T., the HOMEOSTASIS Investigators, 2011. Direct left atrial pressure monitoring in severe heart failure: long-term sensor performance. J. Cardiovasc. Trans. Res. 4, 3–13. https://doi.org/10.1007/s12265-010-9229-z.
Twa, M.D., Roberts, C.J., Karol, H.J., Mahmoud, A.M., Weber, P.A., Small, R.H., 2010. Evaluation of a contact lens-embedded sensor for intraocular pressure measurement. J. Glaucoma 19, 382–390. https://doi.org/10.1097/IJG.0b013e3181c4ac3d.
Vajramani, G.V., Jones, G., Bayston, R., Gray, P.W.P., 2005. Persistent and intractable ventriculitis due to retained ventricular catheters. Br. J. Neurosurg. 19, 496–501. https://doi.org/10.1080/02688690500495299.
Viventi, J., Kim, D.-H., Vigeland, L., Frechette, E.S., Blanco, J.A., Kim, Y.-S., Avrin, A.E., Tiruvadi, V.R., Hwang, S.-W., Vanleer, A.C., Wulsin, D.F., Davis, K., Gelber, C.E., Palmer, L., Van der Spiegel, J., Wu, J., Xiao, J., Huang, Y., Contreras, D., Rogers, J.A., Litt, B., 2011. Flexible, foldable, actively multiplexed, high-density electrode array for mapping brain activity *in vivo*. Nat. Neurosci. 14, 1599–1605. https://doi.org/10.1038/nn.2973.
Weir, R.F., Troyk, P.R., DeMichele, G.A., Kerns, D.A., Schorsch, J.F., Maas, H., 2009. Implantable myoelectric sensors (IMESs) for intramuscular electromyogram recording. IEEE (Inst. Electr. Electron. Eng.) Trans. Biomed. Eng. 56, 159–171. https://doi.org/10.1109/TBME.2008.2005942.
Yetkin, H., Şenköylü, A., Cila, E., Öztürk, A.M., Şimşek, A., 1999. Biodegradable Implants in Orthopaedics and Traumatology.
Yin, L., Cheng, H., Mao, S., Haasch, R., Liu, Y., Xie, X., Hwang, S.-W., Jain, H., Kang, S.-K., Su, Y., Li, R., Huang, Y., Rogers, J.A., 2014a. Dissolvable metals for transient electronics. Adv. Funct. Mater. 24, 645–658. https://doi.org/10.1002/adfm.201301847.
Yin, L., Huang, X., Xu, H., Zhang, Y., Lam, J., Cheng, J., Rogers, J.A., 2014b. Biodegradable electronics: materials, designs, and operational characteristics for fully biodegradable primary batteries (adv. Mater. 23/2014). Adv. Mater. 26 3777–3777. https://doi.org/10.1002/adma.201470152.
Yin, L., Farimani, A.B., Min, K., Vishal, N., Lam, J., Lee, Y.K., Aluru, N.R., Rogers, J.A., 2015. Mechanisms for hydrolysis of silicon nanomembranes as used in bioresorbable electronics. Adv. Mater. 27, 1857–1864. https://doi.org/10.1002/adma.201404579.
Yu, H., Huang, J., 2015. Design and application of a high sensitivity piezoresistive pressure sensor for low pressure conditions. Sensors 15, 22692–22704. https://doi.org/10.3390/s150922692.
Yu, K.J., Kuzum, D., Hwang, S.-W., Kim, B.H., Juul, H., Kim, N.H., Won, S.M., Chiang, K., Trumpis, M., Richardson, A.G., Cheng, H., Fang, H., Thompson, M., Bink, H., Talos, D., Seo, K.J., Lee, H.N., Kang, S.-K., Kim, J.-H., Lee, J.Y., Huang, Y., Jensen, F.E., Dichter, M.A., Lucas, T.H., Viventi, J., Litt, B., Rogers, J.A., 2016. Bioresorbable silicon electronics for transient spatiotemporal mapping of electrical activity from the cerebral cortex. Nat. Mater. 15, 782–791. https://doi.org/10.1038/nmat4624.
Zeng, F., Rebscher, S., Harrison, W., Sun, X., Feng, H., 2008. Cochlear implants: system design, integration, and evaluation. IEEE Rev. Biomed. Eng. 1, 115–142. https://doi.org/10.1109/RBME.2008.2008250.
Zhao, L., Zhang, Z., Song, Y., Liu, S., Qi, Y., Wang, X., Wang, Q., Cui, C., 2016. Mechanical properties and in vitro biodegradation of newly developed porous Zn scaffolds for biomedical applications. Mater. Des. 108, 136–144. https://doi.org/10.1016/j.matdes.2016.06.080.